



ULTIMATE STRAIN CRITERIA AND PLASTIC HINGE LENGTH FOR RC MEMBERS IN MONOTONIC OR CYCLIC FLEXURE

S. Grammatikou⁽¹⁾, D. Biskinis⁽²⁾, M.N. Fardis⁽³⁾

⁽¹⁾ Ph.D. student, Civil Engineering Department, University of Patras, Greece, sofgram@upatras.gr

⁽²⁾ Post-doctoral researcher, Civil Engineering Department, University of Patras, Greece, dbisk@tee.gr

⁽³⁾ Professor, Civil Engineering Department, University of Patras, Greece, fardis@upatras.gr

Abstract

A large volume of measured curvatures in plastic hinges of RC members are used as input to analytical moment-curvature relations to back-estimate strains in rebars and at the extreme concrete fibers of a RC section or its confined core at ultimate conditions due to flexure with axial load. The measurements come from tests on circular or rectangular columns, walls or beams. The ultimate strains derived for rebars and confined or unconfined concrete are not local material properties, as they depend on geometric characteristics of the section and of the immediate neighborhood of its most critical point. The "ultimate" strains show clear size effects: a) the ultimate strain of concrete increases when the size of the compression zone decreases; b) the ultimate strain of tension bars in monotonic loading increases when the number of bars in the tension zone decreases; c) the ultimate strain of steel bars in cyclic loading increases if the number of rebars in the compression zone increases; d) the ultimate strain of confined concrete is larger at a corner of a section subjected to biaxial flexure than along the full side of a rectangular compression zone in uniaxial flexure (along the perimeter of a circular section the ultimate concrete strain is between those of a rectangular section in uniaxial and biaxial bending). For cyclic loading the ultimate strain of bars in tension increases with increasing ratio of bar diameter to stirrup spacing, because the potential for bar buckling in previous compression half-cycles is reduced. The derived ultimate strains apply both as mean values in a plastic hinge and as maximum values at the end section of a prismatic member. Ultimate curvatures computed from the proposed ultimate strains do not have bias and exhibit much less scatter with respect to measured values than those obtained from arbitrary ultimate strains specified in some modern codes; these code predictions are generally unsafe. A much larger volume of experimental measurements, of several hundred cyclic or monotonic tests on rectangular or non-rectangular concrete beams or walls, and circular, rectangular or hollow rectangular columns, is used then to develop expressions for the plastic hinge length of such elements under cyclic or monotonic loading. The expression for circular members is a linear combination of the section's depth and the member's shear span length, times a factor which decreases with increasing axial load level; that for all other types of prismatic concrete members involves an additional factor which depends on the aspect ratio of the section. The so-determined plastic hinge length is to be used in a three-component formula for the ultimate drift capacity of concrete members under monotonic or cyclic loading: the drift ratio at flexural yielding, the fixed-end-rotation of the yielding end due to slippage of the tension bars from their development zone beyond that end and the drift ratio due to the rotation of the plastic hinge. The second and third components are in terms of ultimate curvatures. The expressions for plastic hinge length do not apply, unless the values as ultimate curvatures are those of the paper.

Keywords: concrete members; curvature; displacement-based design; plastic hinge length; strain



1. Introduction

Seismic performance evaluation of existing buildings [1, 2] or of new buildings [3] or bridges [4, 5] normally entails direct checks of seismic deformation demands in ductile, deformation-controlled members against specified limits. Such checks are usually made in terms of plastic hinge rotations [1, 4, 5], or chord rotations at member ends – total or their plastic part [2, 3].

Codes set allowable deformation limits for each performance level. [1] gives tables with allowable plastic hinge rotations in concrete beams, columns or walls, as a function of key parameters and features of the member; it also sets upper limits of 2% to the compressive strain of longitudinal bars (and therefore of the confined concrete) and of 5% to tensile strains of rebars. Chord rotation limits in [2, 3] are derived from the ultimate chord rotation capacity, based either on purely empirical models [6], or on models employing a plastic hinge length – own models in [2] or models by [6] in [3]. In [4] and [5] curvatures and moment-curvature analysis are employed to define the plastic hinge rotation capacity, using the confinement model in [7] – as modified in [8] – for the ultimate strain of confined concrete in [5]. For unconfined concrete, the ultimate strain is set equal to 0.5% in [4] or to 0.4% in [5]. For rebars, [4] adopts two-thirds of the nominal ultimate strain (i.e., 9% for up to 32 mm dia. bars, or 6% for diameters over 36 mm); [5] uses the minimum nominal ultimate strain values of 5% or 7.5% specified in [9] for steel of normal (Class B) or high (Class C) ductility, respectively. By contrast, [2] uses the values of 5% and 6% for these two steel Classes and allows either one of two confinement models: Option 1 is the confinement in Eurocode 2 [9]. Option 2 uses the confinement per [10] and [11] (see Eqs. (3)-(5) below, but with the coefficient 3.5 in Eq.(3) replaced by 3.7 and exponent of 3/4 by 0.86); it also uses an expression of the type of Eqs. (9) for the ultimate strain, but linear in the mechanical ratio of confining reinforcement and the lower limit of Eq. (10) used as unconfined ultimate strain.

It is nowadays recognized that failure or, more generally, ultimate conditions in concrete members, cannot be identified with single local phenomena reflected in material strains. Failure is due to phenomena occurring in a larger region, such as a plastic hinge. Hence, it can be better represented by meso-measures of deformation, such as the overall rotation of a plastic hinge. The renewed interest in local strains has to do with nonlinear analysis models: Strains are convenient deformation measures, if Fiber Models are used to estimate inelastic seismic deformation demands in concrete members. Even when point hinge models are used at member ends, a common practice is to convert their plastic rotation demands to curvatures (by dividing by a postulated plastic hinge length) and employ moment-curvature analysis of the end section to estimate local material strains. However, the ill-supported, almost arbitrary strain limits specified by codes or various researchers are a poor match for a sophisticated analysis. The scientific community of performance-based earthquake engineering has paid so far less attention to the supply side of deformation-based verifications than to the demand side.

The starting point of this work is an analytical link between ultimate curvatures and strains at the extreme concrete fibers of a section or its confined core and at the extreme tension bars. A database of monotonic or cyclic tests in the literature is utilized in order to establish a correspondence between the values of these strains at ultimate conditions of a section (“ultimate strains”) and its mechanical and geometric characteristics. Cyclic tests in which the effects of shear deformation in the plastic hinge were potentially important were identified from their impact on the failure mode of the member as a whole and excluded. Values or expressions for these “ultimate strains” are then derived in terms of these properties. Allowable limits based on these strains can then be compared to strain demands from Fiber Models or from plastic hinge rotations converted to curvatures.

2. Relationship of ultimate curvature and material limit strains

2.1 Ultimate curvature and extreme fiber strains from section analysis

The ultimate deformation (be it the curvature of a section, ϕ , or the chord rotation at one end of a member - alias drift ratio of the member's opposite end) in monotonic or cyclic loading is conventionally identified with the post-ultimate-strength point of the moment-deformation response where the resisting moment, M , cannot increase above 80% of the peak (ultimate) moment with an increase in deformation. The so-defined ultimate curvature, ϕ_u , is the smallest of the values obtained when:



1. Tension bars break at an ultimate elongation ε_{su} ; the ultimate curvature due to steel rupture, φ_{su} , is:

$$\varphi_{su} = \varepsilon_{su} / (d - x_s) \quad (1)$$

where x_s is the neutral axis depth for this type of failure mode and d the effective depth.

2. The extreme compression fibers reach the ultimate strain of concrete, ε_{cu} ; if the neutral axis depth at that point is x_c ; then the ultimate curvature due to concrete crushing, φ_{cu} , is equal to:

$$\varphi_{cu} = \varepsilon_{cu} / x_c \quad (2)$$

If the outcome of Eq.(1) is smaller than that of Eq.(2), it is taken as the ultimate curvature. If it isn't, one has to consider also what happens after the extreme compression fibers reach ε_{cu} and the concrete cover spalls off. Then, only the confined concrete core inside the centerline of the perimeter tie is the active section; Eqs. (1) and (2) are applied anew, using the values of d , x_{su} , x_{cu} of the confined core and the ultimate strain of confined concrete, $\varepsilon_{cu,c}$, instead of ε_{cu} . If the corresponding moment resistance of the confined core, M_{Ro} , exceeds 80% of the moment resistance of the full, unspalled section without the effect of confinement, M_{Rc} , then the minimum outcome of the so-applied Eqs. (1) and (2) is taken as ultimate curvature. If, by contrast, $M_{Ro} < 0.8M_{Rc}$, the outcome of Eq.(2) at spalling of the cover is taken as φ_u .

The values of φ_{cu} , φ_{su} and the associated resisting moment, M_R , can be calculated explicitly by section analysis, as a function of ε_{cu} (or $\varepsilon_{cu,c}$) and ε_{su} , respectively. A portfolio of expressions for x_s , x_c and M_R are given in [12], along with flowcharts for navigation through the lengthy calculation process. In this way a correspondence is established between curvature and extreme fiber strains, which is then inverted to determine the strains at the point when the experimental ultimate curvature is reached (a snapshot of the M - φ curve when M_R drops to 80% of its peak value). This analysis can trace the full M - φ response from the yield point – given, e.g., in [13] or [14, 15] – to the ultimate point. So it is equivalent to a full M - φ analysis, with the reinforcement sectional area smeared along the nearest extreme fibers and with the σ - ε laws described next.

2.2 Material σ - ε laws used in section analysis

For sections with rectangular compression zone, the material σ - ε laws are taken as follows:

- Steel: At the low steel strain accompanying ultimate conditions due to concrete crushing, longitudinal rebars are taken as elastic-perfectly plastic, with yield stress and strain f_y , $\varepsilon_y = f_y / E_s$. At the large strains associated with failure due to steel rupture, rebars are taken to have a yield plateau at the yield stress f_y up to a strain $\varepsilon_{sh} > \varepsilon_y$; then to linearly strain-harden to an ultimate strength point at stress $f_t > f_y$ and elongation $\varepsilon_{su} > \varepsilon_{sh}$.
- Concrete: the σ - ε curve rises as a parabola to the concrete strength f'_c at a strain $\varepsilon_{co} = 0.002$; it stays flat beyond that point up to the “ultimate strain” ε_{cu} .
- Concrete inside stirrups with yield stress f_{yw} and geometric ratio ρ_s (minimum in the two transverse directions), after the extreme compression fibers reach ε_{cu} and the cover spalls: the σ - ε law is again parabolic-rectangular, but with parameters as follows:

- Confined concrete strength, f_{cc} , according to the model in [3], which overall fits test results better than any other confinement model [16]:

$$f_{cc} = f'_c (1 + K), \quad K = 3.5 \left(a \rho_s f_{yw} / f'_c \right)^{3/4} \quad (3)$$

with a : confinement effectiveness [7, 17]:

$$a = (1 - 0.5s_h / b_o) (1 - 0.5s_h / h_o) \left(1 - \sum b_i^2 / (6b_o h_o) \right) \quad (4)$$

In Eq. (4) s_h is the centerline spacing of ties, b_o and h_o the confined core dimensions to the centerline of the perimeter tie, and b_i the distance along that tie between centers of those adjacent bars (index: i) which are engaged by a stirrup corner or cross-tie.

- Strain at f_{cc} per [11] (adopted in [3]), with K from Eq.(3):



$$\varepsilon_{cc} = \varepsilon_{co}(1 + 5K) \quad (5)$$

- Ultimate strain of confined concrete, $\varepsilon_{cu,c}$: It is determined in Section 3.1 from the experimental values of φ_u (see Eqs. (9) and (10)); for $\rho_s f_{yw} = 0$, $\varepsilon_{cu,c}$ is equal to ε_{cu} .

In the compression zone of a circular section, simpler σ - ε laws are used for easier analysis:

- Steel: Elastic-perfectly plastic, with parameters f_y and ε_{su} .
- Concrete: rigid-plastic, as in the rectangular stress block in the upper 80% of the neutral axis depth, $x'=0.8x$, used in flexural design of sections whose width is reduced from the neutral axis to the extreme compression fibers [3]. Till the extreme compression fibers reach the ultimate strain of unconfined concrete, ε_{cu} , the stress of the block is $0.9f'_c$; after spalling, this σ - ε law applies inside the circular hoop, with a constant stress of $0.9f_{cc}$ retained until the ultimate strain of confined concrete, $\varepsilon_{cu,c}$, is reached. Whatever has been said above for the confined concrete in rectangular compression zones applies, using in Eq.(3) $\rho_s = 2A_{sw}/(D_o s_h)$, where A_{sw} is the cross-sectional area of a circular hoop with centerline diameter D_o . Eq.(4) is replaced by:

$$a = (1 - 0.5s_h/D_o)^n \quad (6)$$

where $n = 2$ for individual circular hoops or $n = 1$ for spiral reinforcement.

For square sections loaded along the diagonal:

- Steel: The same as in sections with rectangular compression zone.
- Concrete: The same as for circular sections, but with effective confinement as in sections with rectangular compression zones, Eq. (4).

If f_{cc} and ε_{cc} are taken according to the models above, the free parameters available to fit the experimental values of φ_u are the ultimate strains of steel, ε_{su} , and confined concrete, $\varepsilon_{cu,c}$, examined separately for monotonic or cyclic loading, different shapes of compression zone and number and layout of longitudinal bars.

2.6 Effect of slippage of tension bars from their anchorage past the end section

Curvatures at or near the critical end section are often derived from relative rotation with respect to another section, divided by the distance between these sections. If the rotation is measured from the face of the anchoring block (e.g., of a specimen's footing), it includes the fixed-end-rotation of the end section due to slippage of the longitudinal bars from their development and toward the body of the specimen. This rotation component should be removed from the measured total rotation. According to tests and theory, at yielding of the end section the fixed-end-rotation is $\theta_{y,slip} = d_{bL} f_{y1} \varphi_y / (8\sqrt{f'_c})$, where d_{bL} is the mean diameter of tension bars, f_{y1} their yield stress, φ_y the curvature of the end section at yielding and f'_c , f_{y1} are in MPa [14]. After yielding of the end section and till the ultimate curvature occurs there, inelastic strains penetrate into the development zone of tension bars past the end section, increasing further the fixed-end rotation due to bar slippage.

In 168 cases out of those used in this paper for the derivation of ultimate strains from curvatures, relative rotations measured at different gauge lengths include this fixed-end rotation. On the basis of these data, the additional fixed-end rotation between yielding and ultimate curvature was inferred as equal to:

$$\text{– For cyclic loading:} \quad \Delta\theta_{u,slip} = 4.5d_{bL}\varphi_u \quad (7a)$$

$$\text{– For monotonic loading:} \quad \Delta\theta_{u,slip} = 10d_{bL}\varphi_u \quad (7b)$$

Eqs. (7) imply that the bars are perfectly-plastic along a yield-penetration-length equal to the multiple of d_{bL} in these expressions. About as good fit to the data is achieved if the bars are taken as linearly strain-hardening all along that length and $(\varphi_y + \varphi_u)/2$ is used in lieu of φ_u :

$$\text{– For cyclic loading:} \quad \Delta\theta_{u,slip} = 4.25d_{bL}(\varphi_u + \varphi_y) \quad (8a)$$



– For monotonic loading:
$$\Delta\theta_{u,slip} = 9d_{bL}(\varphi_u + \varphi_y) \quad (8b)$$

For circular sections, those with rectangular compression zone, or square sections loaded along the diagonal, expressions for φ_y for use in Eqs. (8) are given in [15, 14] and [12], respectively.

Once curvatures are corrected for the effect of the fixed-end rotation per Eqs. (7) or (8), there is no bias in the measured curvature due to the gauge length.

3. Strain criteria at the ultimate curvature of the section

3.1 Extreme fiber strains estimated from experimental ultimate curvatures

The correspondence between φ_u and ε_{su} or $\varepsilon_{cu,c}$ per Section 2 was inverted to back-estimate strains from the experimental curvature at flexure-controlled failure of the member end. For each possible failure mode (i.e., due to rupture of tension bars, crushing of the concrete core, cover spalling) plots of these “experimental” strains against the relevant independent geometric or material variables revealed any statistically significant dependence and suggested suitable mathematical forms to express it. The coefficients in these expressions were estimated via multiple nonlinear regressions and modified to obtain unbiased, minimum variance estimates of the experimental curvatures.

Three cases were considered regarding the measurements:

1. All measurements of curvature in a test, taken over different gauge lengths from the end section, are considered with the same weight. This is equivalent to using the mean curvature over a member end region, weighted by the number of gauge lengths in the test.
2. The average curvature over the member’s end region is used for each test, with a weight of 1.0 for each test.
3. Only one curvature in each test is used: the one measured closest to the end section.

Cases 1 and 2 give essentially the same estimates of ε_{su} , $\varepsilon_{cu,c}$, summarized below as case (a); case 3 is then renamed to (b).

(a) Ultimate strains from the mean value of ultimate curvature over the plastic hinge region:

For concrete, extreme fiber strains back-estimated from ultimate curvatures were found to depend on: a) the compression zone shape and size (at least for small sizes) and b) confinement - expressed as the product of the confinement effectiveness factor, a , per Eqs. (4) or (6), the volumetric ratio of transverse steel, ρ_w , and the ratio of its yield stress, f_{yw} , to f'_c : $\omega_w = \rho_w f_{yw} / f'_c$. The more numerous data for sections with rectangular compression zone suggest a square-root-type of dependence on $a\omega_w = a\rho_w f_{yw} / f'_c$. The same type of dependence was adopted for the much fewer cyclic tests of circular or diagonally tested members. The least-squares fitting of this functional form gave the following expressions for the ultimate strain of confined concrete, $\varepsilon_{cu,c}$.

- rectangular compression zone:
$$\varepsilon_{cu,c} = \varepsilon_{cu} + 0.04\sqrt{a\rho_w f_{yw} / f'_c} \quad (9a)$$

- circular section (cyclic loading):
$$\varepsilon_{cu,c} = \varepsilon_{cu} + 0.07\sqrt{a\rho_w f_{yw} / f'_c} \quad (9b)$$

- triangular compression zone (cyclic loading):
$$\varepsilon_{cu,c} = \varepsilon_{cu} + 0.12\sqrt{a\rho_w f_{yw} / f'_c} \quad (9c)$$

Eq. (9a) was fitted to monotonic and cyclic test results together, as differences between them are not systematic and cannot support separate expressions; however, having a common expression increases the scatter of the data with respect to it. In contrast, Eqs. (9b) and (9c) were fitted to cyclic tests alone; strictly speaking they apply only to cyclic loading. Eq. (9a) applies to uniaxial flexure; Eq. (9c) to biaxial, which concentrates compressive stresses and strains at one corner of the section and its vicinity. Because Eqs. (9) refer exclusively to the extreme compression fibers at the instant of ultimate curvature of a section under flexure with or without axial load; they give higher values than expressions fitted to concentric compression tests (e.g., [7]).



The data clearly show that the ultimate strain of unconfined concrete, ε_{cu} , back-estimated from the ultimate curvature, increases with decreasing section size. If h_o and d_o denote the depth and the effective depth, respectively, of the confined core (taken equal to those of the full section at spalling of the extreme compression fibers), this size-effect may be described by the following expression:

$$0.0035 \leq \varepsilon_{cu} = \left(18.5 / h_o(mm)\right)^2 \leq 0.01, \quad (10)$$

The size effect vanishes for the sizes found in practice; for them ε_{cu} comes out equal to 0.0035.

Concerning the tension bars, strains back-estimated from ultimate curvatures depend on: a) the loading (monotonic or cyclic), b) the number of bars in a certain zone of the section and c) (in some cases) the bar-diameter-to-stirrup-spacing ratio. Best fit was achieved with the following expressions for the ultimate strain of tension bars, ε_{su} :

– for monotonic loading:
$$\varepsilon_{su,mon} = \left(1 - 0.3\sqrt{\ln N_{b,tens}}\right) \varepsilon_{su,nom} \quad (11a)$$

– in cyclic loading, before the cover spalls:
$$\varepsilon_{su,cy} = 0.4\varepsilon_{su,nom} \quad (11b)$$

– cyclic loading, after spalling:
$$\varepsilon_{su,cy} = (4/15)\varepsilon_{su,nom} \left(1 + 3d_{bL} / s_h\right) \left(1 - 0.75e^{-0.4N_{b,compr}}\right) \quad (11c)$$

where $\varepsilon_{su,nom}$ is the uniform elongation at tensile strength in a standard steel coupon test and $N_{b,tens}$, $N_{b,compr}$ denote the number of tension bars, or of those at the extreme compression fibers, respectively. In rectangular sections subjected to uniaxial bending $N_{b,tens}$ corresponds to the tension reinforcement; in circular sections to that in the entire tension zone. In rectangular sections and uniaxial bending $N_{b,compr}$ corresponds to the compression reinforcement; it is 1 in diagonally loaded sections (one corner bar) and taken equal to 2 in circular sections.

(b) Ultimate strains derived from the ultimate curvature measured closest to the end section:

The differences with case (a) above were not so large as to justify major changes in the strain limits. The only worthy change is to use $N_{b,compr} = 4$ for circular sections in Eq. (11c).

The reason for the significant difference of $\varepsilon_{su,mon}$ from $\varepsilon_{su,nom}$ is statistical, similar to the size effect in brittle materials (see Eqs. (10) for the present case). The monotonic tests in the database with rupture of the tension steel had from one to 9 bars in the tension zone; they exhibit a statistically significant reduction of ε_{su} at ultimate curvature with increasing $N_{b,tens}$, because it is the minimum value of ε_{su} among these bars that controls failure. The functional form of Eq. (11a) (linear in $\sqrt{\ln N}$) is not the one that fits best the data in Fig. 1; it is derived per [18] as the mode (i.e., most likely value) in a Type-I extreme value probability distribution of the smallest ε_{su} -value in N bars, all of which have a mean ε_{su} -value of $\varepsilon_{su,nom}$. The parameters of the linear dependence are then fitted to the test data (Eq. (11)).

Under cyclic loading a bar breaks in tension after it has buckled in a previous half-cycle. Buckling produces microcracks at the root of ribs, which spread and precipitate fracture when the bar is stretched in a tensile half-cycle. Closely spaced ties reduce bar slenderness and delay buckling. Slenderness is expressed in Eqs. (11) by the tie-spacing-to-bar-diameter ratio, s_h/d_{bL} : a value of s_h/d_{bL} equal to 5 increases ε_{su} by 28%, compared to the value for $s_h/d_{bL}=12$. The improvement of ε_{su} at low s_h/d_{bL} values is not dramatic: the reason is that a low value delays buckling, but increases the curvature imposed – under axial deformation control – on the bar once it buckles, promoting the microcracking which leads to rupture.

Delay of buckling is also the reason for the improvement of ε_{su} with increasing number of bars at the extreme compression fibers. Before they buckle, these bars share with the member its curvature in the longitudinal direction, hence their convex side faces inwards. For them to buckle outwards, this curvature has to be reversed. This effect delays buckling of intermediate bars but lets the corner ones buckle sideways. So, ε_{su} increases with increasing number of compression bars. Intermediate bars improve confinement of the concrete core and delay the disintegration that sets these bars free to buckle inwards.



The marked scatter of the extreme fiber strains back-calculated from ultimate experimental curvatures with respect to the fitted expressions reflects the sizeable scatter intrinsic in curvature measurements, as well as random local factors and phenomena having little impact on the ultimate deformation of the section.

3.2 Comparison of experimental ultimate curvatures with calculated values

Fig. 1 compares the experimental ultimate curvatures at all sections in the database (option 1 in Section 3.1) with the ones calculated using the values of ε_{su} and ε_{cu} in Section 3.1.

Table 1: Statistics of the measured-to-calculated ultimate curvature ratio

$\varphi_{u,exp}/\varphi_{u,pred}$ for different testing conditions or failure modes		single value of curvature per test						all measurements in a test given same weight				
		# of tests	near end section			mean in plastic hinge			# of data	mean	Media n	CoV %
			Mean	median	CoV %	mean	median	CoV %				
1	All tests, with proposed ultimate strain	410	1.08	1.01	48.7	1.06	0.98	48.3	645	1.05	0.99	45.8
2	Monotonic tests, rectangular or circular sections	226	1.05	0.98	47.3	1.04	0.96	46.9	271	1.03	0.97	45.7
3	Cyclic tests, rectangular, circular, or diagonal cases	184	1.115	1.03	50.0	1.08	1.00	49.8	374	1.06	1.00	45.8
4	No bar slippage from anchorage zone	288	1.11	1.03	48.2				477	1.06	0.99	47.4
5	With bar slippage from anchorage	122	1.00	0.96	49.4				168	0.99	0.96	47.4
6	Rectangular sections, all failure modes (below); cyclic tests	151	1.07	1.01	50.5	1.06	0.99	49.8	272	1.06	0.99	44.4
7	Cover spalls in full rectangular section	59	1.06	1.03	39.6	1.06	1.03	39.8	65	1.06	1.03	38.8
8	Confined core crushes; monotonic uniaxial tests	107	1.00	0.90	47.2	1.00	0.90	47.2	107	1.00	0.90	47.2
9	Confined core crushes; cyclic uniaxial tests	79	1.05	0.96	49.0	1.045	0.96	46.7	121	1.05	0.96	46.3
10	tension bars break; monotonic uniaxial tests	59	1.13	1.05	53.2	1.10	1.02	52.7	97	1.05	1.00	48.8
11	tension bars break before spalling; cyclic uniaxial tests	15	0.975	0.90	34.0	1.015	0.96	34.5	40	1.07	1.00	30.8
12	tension bars break after spalling; cyclic uniaxial tests	56	1.06	1.04	39.9	1.04	1.01	40.9	110	1.04	1.03	36.8
13	Circular section, concrete crushed, monotonic or cyclic tests	10	1.09	1.07	38.6	1.09	1.095	41.6	20	1.09	1.07	47.2
14	Circular section, steel rupture; cyclic	20	1.15	1.01	49.0	1.2	1.01	55.2	72	1.05	0.98	49.7
15	Square section; concrete crushed, cyclic diagonal tests	4	1.15	1.12	10.6	1.08	1.04	32.2	12	0.99	1.05	33.3
16	Limit strains in CEN (2005a) option 1; cyclic tests	184	1.44	1.16	61.5	1.42	1.15	62.6	374	1.36	1.15	59.7
17	Limit strains in CEN (2005a) option 2; cyclic tests	184	0.93	0.80	57.0	0.91	0.76	57.1	374	0.93	0.80	54.5
18	Limit strains in Caltrans (2006); cyclic	184	0.99	0.81	67.9	0.97	0.78	69.6	374	0.93	0.73	71.9
19	Limit strains in CEN (2005b); cyclic	184	1.03	0.88	66.2	1.00	0.86	65.7	374	1.07	0.88	64.2

* If the sample size is large, the median is more representative of the average trend than the mean value.

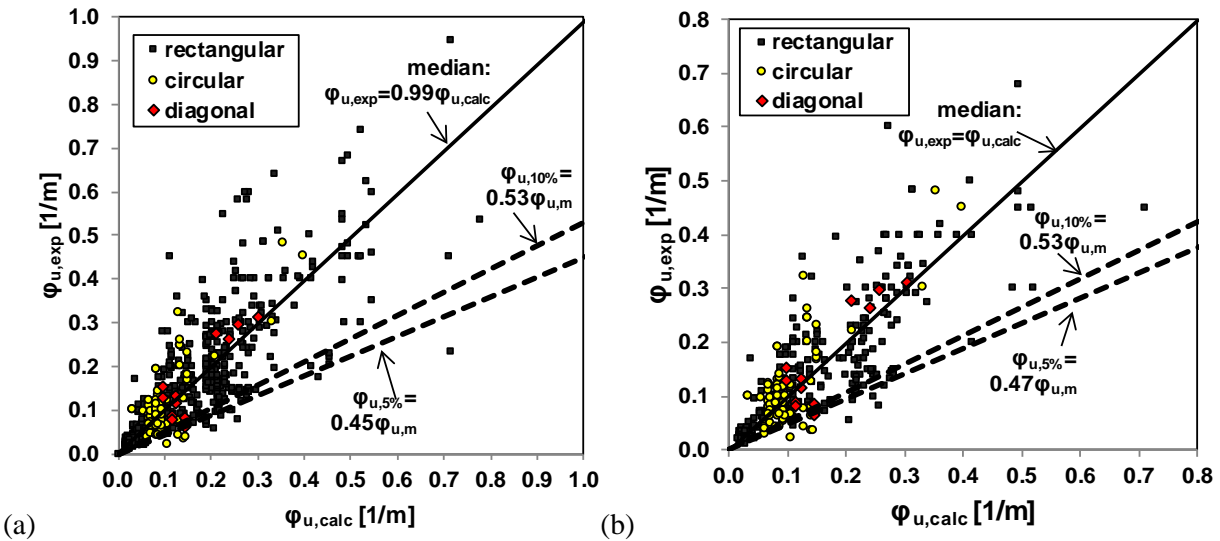


Fig. 1 – Experimental ultimate curvatures vs. calculated using proposed ultimate strains for: (a) monotonic and cyclic tests; (b) cyclic tests, separately.

Table 1 gives statistics of the measured-to-calculated-value ratio per failure mode, using in the calculation the results of Section 3.1 for ε_{su} , $\varepsilon_{cu,c}$: rows 6 to 12 refer to sections with rectangular compression zone, rows 13 and 14 are for circular sections and row 15 for square sections tested diagonally. Statistics are also given separately for monotonic or cyclic loading (rows 2 and 3), and for cases with or without bar slippage from its anchorage beyond the member end (rows 4 and 5). In all separate cases, as well as overall (row 1), the median is equal, or very close, to 1.00. The statistics are better when all measurement stations are included with the same weight, no matter their number. The coefficients of variation, overall (in row 1) and for each separate case, are lower than for members with rectangular compression zone in [6] – see Table 2 therein. Note that [6] proposed fixed values of $\varepsilon_{su}/\varepsilon_{su,nom}$, equal to 3/8 or 7/12 for cyclic or monotonic loading, respectively, $\varepsilon_{cu} = 0.0035$ for unconfined concrete and a stronger effect of confinement.

Fig. 2 compares experimental values for cyclic loading with those computed from the strain limits quoted in the introduction for three standards: [2] or [5] and [4]. The last four rows of Table 1 give statistics of the ratio of the experimental values to those predictions. The scatter in Fig. 2 is much larger than in Fig. 1(b) and, more important, there is considerable bias. The bias is mostly due to the strain limits for rebars in these standards, which are significantly larger than the values from Eqs. (11). The concrete ultimate strains in [4] and [5] are safe-sided compared to the outcomes of Eqs. (9), (10); the one in [9] – adopted as first option in [2] – is even more so. In contrast, the second ultimate strain option in [2] is unsafe compared to Eq. (9a).

As demonstrated in Fig. 2(a) and the 4th row from the bottom of Table 1, only in option 2 in [2] the safe-sided concrete ultimate strain makes up for the unconservative steel strain limits. By contrast, the ultimate curvatures from option 2 in [2] and from [5] or [4] are unsafe.

Experimental curvatures were corrected for the effect of fixed end rotation before comparing them with predictions in Figs. 1 and 2 or computing the statistics in Table 1.

4. Flexure-controlled ultimate drift ratio from ultimate curvature and plastic hinge length

In a physical model of post-elastic flexure of the shear span, L_s , next to a member end, inelastic flexural deformations are lumped in a plastic hinge length, L_{pl} , measured from the end which has yielded. The rest of the shear span is considered as elastic. The inelastic part of the curvature, $(\varphi - \varphi_y)$, is taken as constant along the plastic hinge length and as zero outside. A post-elastic fixed-end rotation, $\Delta\theta_{slip}$, develops after yielding of the end section, owing to penetration of yielding in the development length of the tension bars past beyond the member end. The ultimate value of the drift ratio of the shear span - defined as the deflection of the end of the shear span with respect to the tangent to the member axis at the yielding end - is the same as the ultimate value



of the chord rotation of the yielding end - angle between the tangent to the member axis at the yielding end and the chord connecting the two ends; they are both denoted as θ_u and take place when the curvature, ϕ , attains its ultimate value, ϕ_u . By then $\Delta\theta_{slip}$ has increased to $\Delta\theta_{u,slip}$, given by Eqs. (7) or (8). So:

$$\theta_u = \theta_y + (\phi_u - \phi_y)L_{pl}\left(1 - 0.5L_{pl}/L_s\right) + \Delta\theta_{u,slip} \quad (12)$$

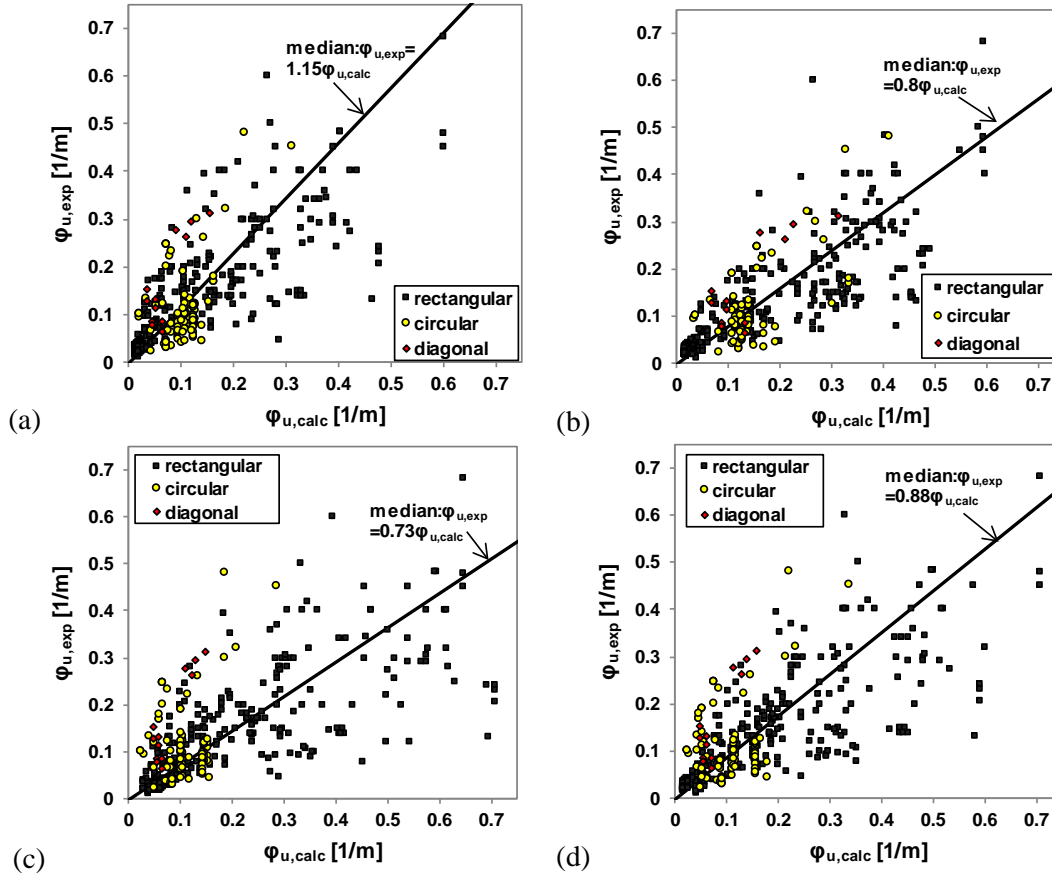


Fig. 2 – Experimental ultimate curvatures in cyclic loading vs. predictions for limit strains per (a) [2], option 1: confinement model per [9]; (b) [2] with option 2: own confinement model; (c) [4]. (d) [5].

For ϕ_u computed per Section 3 above, the chord rotation at yielding, θ_y , and the yield curvature, ϕ_y determined per [14, 15, 19] and $\Delta\theta_{u,slip}$ from Eqs. (7) or (8), the following expressions for L_{pl} were fitted in the present work to the measured ultimate chord rotations in few thousands of flexure-controlled tests in the database:

- For beams or columns with section of rectangular parts, walls of all types and hollow piers.
 - For monotonic loading:

$$L_{pl} = 0.34h \left(1 + 1.1 \min \left(9, \frac{L_s}{h} \right) \right) \left(1 - \frac{1}{2} \sqrt{\min \left(2.5, \max \left(0.05, \frac{b_w}{h} \right) \right)} \right) \left(1 - \frac{1}{2} \min (0.7, v) \right) \quad (13a)$$

- For cyclic loading:

$$L_{pl} = 0.3h \left(1 + 0.4 \min \left(9, \frac{L_s}{h} \right) \right) \left(1 - \frac{1}{3} \sqrt{\min \left(2.5, \max \left(0.05, \frac{b_w}{h} \right) \right)} \right) \left(1 - 0.45 \min (0.7, v) \right) \quad (13b)$$

- For columns with circular section, in cyclic loading:



$$L_{pl} = 0.7D \left(1 + \frac{1}{7} \min \left(9, \frac{L_s}{D} \right) \right) (1 - \min(0.7, v)) \quad (14)$$

In Eqs. (13) and (14):

- h (D in circular sections): section depth
- $L_s=M/V$: shear span at the section of maximum moment;
- b_w : web width (m);
- $v=N/A_c f'_c$ with A_c : cross-sectional area and N : axial force, positive for compression.

The format of Eqs. (13), (14) shows that the common practice of taking the plastic hinge length as a multiple or fraction of the section's depth is not sufficient: it increases also with increasing shear span ratio, at least up to a certain limit, and decreases with increasing axial load ratio.

Fig. 3 compares the experimental flexure-controlled ultimate chord rotation or drift ratio to the predictions per this Section. Statistics of the test-to-prediction ratio are listed in Table 2.

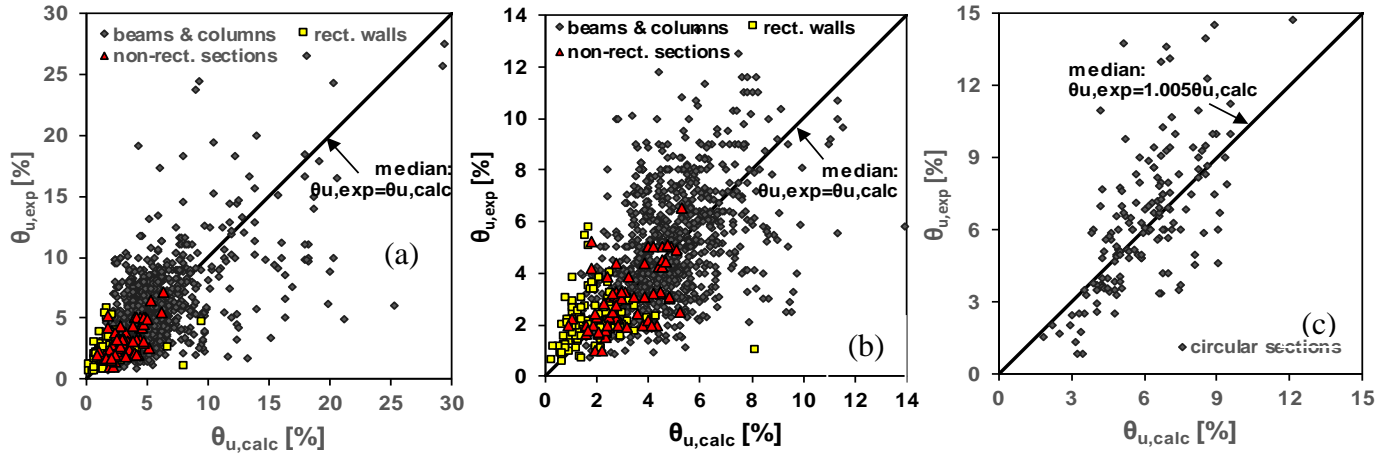


Fig. 3 Ultimate chord rotation, test v prediction of Eqs.(12)-(14): (a) rectangular beams, columns, walls, all sections except circular, monotonic loading; (b) ibid, cyclic loading; (c) circular columns, cyclic loading

Table 2 Statistics of test-to-prediction ratio of flexure-controlled ultimate chord rotation of members, conforming or not, with continuous bars, deformed or plain

		# of tests	mean*	median*	CoV
1	all members except circular	1499	1.13	1.00	52.6%
2	all members except circular; monotonic tests	301	1.22	1.00	71.2%
3	all members except circular; cyclic tests	1198	1.1	1.00	45.1%
4	all members except circular, no bar slippage	203	1.26	1.03	64.4%
5	all members except circular, with bar slippage	1296	1.11	1.00	49.6%
6	rectangular or non-rectangular walls and hollow piers, with bar slippage	211	1.20	1.01	51.7%
7	circular columns with bar slippage	157	1.055	1.005	34.8%

* footnote of Table 1 applies

5. Conclusions

A large number of experimental measurements of curvatures in the plastic hinge region of concrete members are combined with analytical moment-curvature relationships to back-estimate the strain at the extreme concrete fiber of a section or its confined core and the strain in the tension bars, which correspond to the ultimate condition of a concrete section subjected to flexure with axial load. Strain limits derived from these “ultimate”



strains can support nonlinear analyses with Fiber Models or with member models employing plastic hinges of finite length at each end and curvatures. The experimental data are drawn from a large number of tests of circular or rectangular columns (some tested diagonally), walls or beams.

The ultimate strains derived exhibit clear size effects:

- That of concrete increases with decreasing compression zone (see Eq. (10));
- The one of tension bars for monotonic loading decreases with increasing number of bars in the tension zone (see Eq. (11a)).
- The cyclic ultimate strain of steel reinforcement after spalling increases with increasing number of bars in the compression zone (see Eq. (11c))
- The increase of the concrete ultimate strain thanks to confinement is larger at the corners of a section subjected to biaxial bending than all along the side of a rectangular compression zone under uniaxial flexure; the increase at the perimeter of a circular section is in-between these two extreme (cf. Eqs. (9)).

The ultimate strain of rebars in tension for cyclic flexure increases with increasing bar-diameter-to-stirrup-spacing ratio, thanks to prevention or delay of bar buckling in a preceding compression half-cycle (see Eq. (11c)). This point, as well as all bullet points above, confirm that, under flexure with axial load (especially of the cyclic type), the ultimate strain of steel or concrete is not a local material property but depends on geometric features of the whole RC section and of the immediate vicinity of the most critical point in the section. This effect has long been recognized, but not quantified in a systematic way. So, to the present day, strain limit criteria have not explicitly taken it into account.

Essentially the same ultimate strains apply to the plastic hinge as a whole or to the end section of a prismatic member.

The data suggest lower ultimate strains of rebars under cyclic loading than in monotonic. By contrast, there is little experimental evidence of a reduction in the ultimate strain of confined concrete due to load cycling.

The ultimate curvatures calculated using the proposed ultimate strains are unbiased and have much less prediction scatter than those obtained from the arbitrary and generally unsafe ultimate strains specified in various codes for the seismic evaluation of concrete structures. The scatter with respect to the calculated curvatures has been quantified; it may be taken into account in design by using 5%- or 10%-fractile values of the curvature, which are around 50% of the estimates calculated as per this work.

A much larger number of cyclic or monotonic tests on rectangular or non-rectangular concrete beams or walls, and circular, rectangular or hollow rectangular columns, provided the basis for expressions giving the plastic hinge length of such elements under cyclic or monotonic loading. The expression for circular members is a linear combination of the section's depth and the member's shear span length, times a factor which increases with increasing axial load level. The expression for all other types of prismatic concrete members involves an additional factor which depends on the aspect ratio of the section. The so-determined plastic hinge length is to be used in a three-component formula for the ultimate drift capacity of concrete members under monotonic or cyclic loading: a) the drift ratio at flexural yielding, b) the fixed-end-rotation of the yielding end due to slippage of the tension bars from their development zone beyond that end, and c) the drift ratio due to the rotation of the plastic hinge. The second and third components are in terms of ultimate curvatures. The common practice of taking the plastic hinge length as a multiple or fraction of the section's depth is wanting: the plastic hinge length increases also with increasing shear span ratio, at least up to a certain limit, and drops with increasing axial load ratio. For monotonic loading, not only the ultimate strain limits are higher than for cyclic, but also the plastic hinge length is longer.

The expressions developed for the plastic hinge length do not apply, unless the values used as ultimate curvatures are those of the paper.



6. Acknowledgements

The research leading to these results receives funding from the General Secretariat for Research and Technology, grant ERC-12 of the Operational Program "Education and lifelong learning", co-funded by the European Union (European Social Fund) and national resources.

7. References

- [1] ASCE (2007). Seismic rehabilitation of existing buildings. ASCE Standard ASCE/SEI 41-06, American Society of Civil Engineers, Reston, VA.
- [2] CEN (2005a) European Standard EN 1998-3:2005: Eurocode 8: Design of structures for earthquake resistance. Part 3: Assessment and retrofitting of buildings. Comité Européen de Normalisation. Brussels.
- [3] *fib* (2012) Model Code 2010, Final draft. Bulletin 65/66, Federation Internationale du Beton, Lausanne
- [4] CALTRANS (2006) Seismic Design Criteria, Version 1.4 Caltrans, Sacramento, CA.
- [5] CEN (2005b) European Standard EN 1998-2:2005 Eurocode 8: Design of structures for earthquake resistance. Part 2: Bridges. Comité Européen de Normalisation. Brussels.
- [6] Biskinis, D. and Fardis, M.N. (2010b) Flexure-controlled ultimate deformations of members with continuous or lap-spliced bars. *Struct. Concrete*, 11(2), 93-108.
- [7] Mander, J.B., Priestley, M.J.N. and Park, R. (1988) Theoretical stress-strain model for confined concrete. *ASCE, J. Struct. Eng.*, 114(8): 1804-1826.
- [8] Paulay, T. and Priestley, M.J.N. (1992) *Seismic design of reinforced concrete and masonry buildings* J.Wiley, New York, N.Y.
- [9] CEN (2004) European Standard EN 1992-1-1:2004: Eurocode 2: Design of concrete structures. Part 1-1: General rules and rules for buildings. Comité Européen de Normalisation. Brussels.
- [10] Newman, K. and Newman, J.B. (1971) *Failure theories and design criteria for plain concrete*. In (Te'eni ed) *Structure, Solid Mechanics & Engineering Design* J.Wiley, New York, N.Y.
- [11] Richart, F.E., Brandtzaeg, A. and Brown, R.L. (1928) A study of the failure of concrete under combined compressive stresses, Bull. 185, Un. Illinois Eng Exp Station, Champaign, ILL
- [12] Grammatikou, S., Biskinis, D. and Fardis M.N. (2016). Ultimate strain criteria for RC members in monotonic or cyclic flexure. *J. Struct. Eng. ASCE*, 142, DOI: 10.1061/(ASCE)ST.1943-541X.0001501 (On line, March 22, 2016).
- [13] Panagiotakos, T.B. and Fardis, M.N. (2001) Deformations of RC members at yielding and ultimate. *ACI Struct. J.* 98(2): 135-148
- [14] Biskinis, D. and Fardis, M.N. (2010a) Deformations at flexural yielding of members with continuous or lap-spliced bars. *Struct. Concrete*, 11(3), 127-138.
- [15] Biskinis, D. and Fardis, M.N. (2013) Stiffness and cyclic deformation capacity of circular RC columns with or without lap-splices and FRP wrapping *Bull. Earthq Eng.* 11(5) 1447-1466
- [16] Fardis, M.N. (2013) Performance- and displacement-based seismic design and assessment of concrete structures in the Model Code 2010. *Struct. Concrete*, 14(3), 215-229
- [17] Sheikh, S.A. and Uzumeri, S.M. (1982) Analytical model for concrete confinement in tied columns. *ASCE, J. Struct. Eng.*, 108(ST12), 2703-2722.
- [18] Benjamin, J.R. and Cornell, C.A. (1970) *Probability, statistics and decision for Civil Engineers* McGraw Hill, New York, N.Y.
- [19] Grammatikou, S., Biskinis, D. and Fardis M.N. (2015) Strength, deformation capacity and failure modes of RC walls under cyclic loading *Bull. Earthq. Eng.* Vol. 13(11) 3277-3300.